not bind to the cluster. However, the enzyme also is *able* to accommodate substrate bound by the α-carboxyl, as is shown by ^{17}O ENDOR of enzyme that has bound a ^{17}O-enriched isocitrate analogue that lacks the β-carboxyl. Presumably the addition of the negatively charged carboxyl causes protonation of the OH^- that binds to the cluster in the absence of substrate.

The resulting ENDOR-derived structure for the substrate-bound cluster (Figure 8) is remarkably well corroborated by recent X-ray diffraction information.[34b] As seen by ENDOR spectroscopy, the cluster appears to function as follows: (i) it helps to position the substrate through the binding of one carboxyl; (ii) it coordinates and accepts the hydroxyl of substrate during the dehydration of citrate and isocitrate; (iii) it donates a bound hydroxyl during the rehydration of *cis*-aconitate. Further, to accommodate the stereochemistry of the reaction, *cis*-aconitate must disengage from the active site, rotate 180°, and switch the carboxyl that binds before completing the catalytic cycle.

Conclusion

The few examples presented above have been selected from among many (Table I) to illustrate how the ENDOR technique can answer questions about metalloenzyme structure and function that have resisted other means of approach. An implicit aspect has been the importance of precise isotope labeling as well as our development of procedures for the analysis of frozen-solution ENDOR spectra and of multifrequency capabilities. Work in progress[35] shows that there are further benefits to the utilization of pulsed-ENDOR techniques[36] in addition to CW ENDOR. In short, it is easy to envision continued expansion of the role played by ENDOR spectroscopy in the study of metallobiomolecules.

In addition to collaborators mentioned above, others associated with projects that could not be mentioned are equally acknowledged, as are the graduate students and postdoctorals whose work is described here. These studies could not have been performed without the technical expertise of Mr. Clark E. Davoust or the support of the NIH, NSF, and USDA.

(35) Doan, P.; Fan, C.; Davoust, C. E.; Hoffman, B. M. *J. Magn. Reson.*, submitted.
(36) *Modern Pulsed and Continuous Wave Electron Spin Resonance*; Kevan, L., Bowman, M. K., Eds.; Wiley: New York, 1990.

Scanning Tunneling Microscopy Studies of Low-Dimensional Materials: Probing the Effects of Chemical Substitution at the Atomic Level

CHARLES M. LIEBER* and XIAN LIANG WU

Department of Chemistry, Columbia University, New York, New York 10027

Received January 23, 1991 (Revised Manuscript Received April 15, 1991)

A major goal of current research efforts in solid-state chemistry and physics is to understand the factors that determine the electronic and structural properties and phase transitions in materials.[1,2] This understanding is essential to the materials sciences since it will lead the way to the rational design and preparation of new solids with predictable properties. A general experimental approach that has been used to probe these factors involves studies of chemically substituted or doped materials.[3-6] Substitutional doping is a useful technique since it can affect systematic variations in the carrier density of a material and, for example, convert a semiconductor to a metal or tune the properties of a metal so that it will become a superconductor. Substitutional doping will also cause disorder in the lattice which can lead to a metal–insulator transition.[6] It is important for new materials design to predict which of these manifestations of doping will dominate.

In the past, the electronic effects of substitutional doping have been investigated by photoelectron and optical spectroscopies and transport measurements, while structural manifestations of doping have been probed by X-ray, neutron, and electron diffraction

Charles M. Lieber received a B.A. with honors in chemistry from Franklin and Marshall College in 1981. He received a Ph.D. from Stanford University in 1985, working with Nathan Lewis on kinetic and catalytic studies of modified electrodes, and then moved to Caltech to pursue postdoctoral research on long-range electron transfer in metalloproteins with Harry Gray. In 1987 he joined the faculty of Columbia University, and he was promoted to Associate Professor of Chemistry in 1990. His current research interests include the chemical physics of solids and interfaces, especially high-temperature superconductivity, charge density waves, and the atomic origins of friction.

Xian Liang Wu received a B.S. from Peking University in 1982 and an M.S. from Hebei University in 1985. He is currently completing a Ph.D. on scanning tunneling microscopy studies of low-dimensional materials with Charles Lieber.

(1) DiSalvo, F. J. *Science* **1990**, *247*, 649.
(2) (a) *Physics Through the 1990s: Condensed-Matter Physics*; National Academy Press: Washington, 1986. (b) *Physics Through the 1990s: Scientific Interfaces and Technological Applications*; National Academy Press: Washington, 1986.
(3) Miller, J. S.; Epstein, A. J. *Angew. Chem., Int. Ed. Engl.* **1987**, *26*, 287.
(4) (a) Rao, C. N. R.; Raveau, B. *Acc. Chem. Res.* **1989**, *22*, 106. (b) Sleight, A. W. *Science (Washington)* **1988**, *242*, 1519. (c) Williams, J. M.; Beno, M. A.; Carlson, K. D.; Geiser, U.; Kao, H. C. I.; Kini, A. M.; Porter, L. C.; Shultz, A. J.; Thorn, R. J.; Wang, H. H. *Acc. Chem. Res.* **1988**, *21*, 1.
(5) (a) Dresselhaus, M. S.; Dresselhaus, G. *Adv. Phys.* **1981**, *30*, 139. (b) Zabel, H.; Chow, P. C.; *Comments Solid State Phys.* **1986**, *12*, 225. (c) Ebert, L. B. *Annu. Rev. Mater. Sci.* **1976**, *6*, 181.
(6) DiSalvo, F. J.; Wilson, J. A.; Bagley, B. G.; Waszczak, J. V. *Phys. Rev. B* **1975**, *12*, 2220.

0001-4842/91/0124-0170$02.50/0

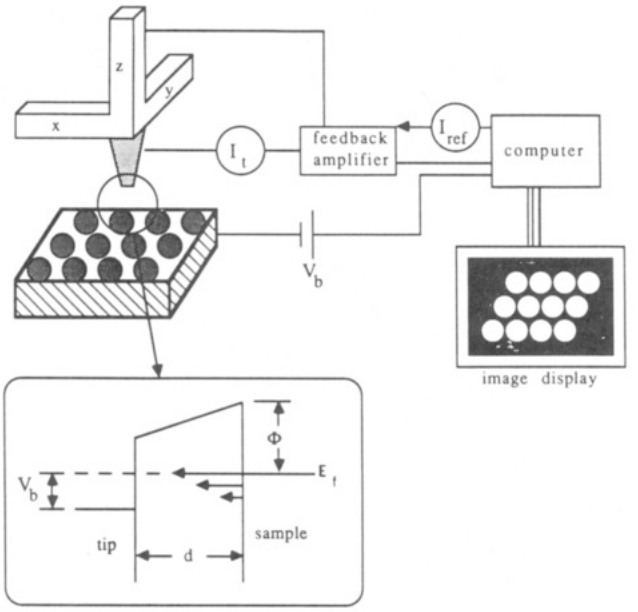

Figure 1. Schematic view of the scanning tunneling microscope. The x–y–z map of the surface is displayed as a "gray scale" where light corresponds to raised surface features. The inset is a one-dimensional representation of tunneling between a metallic tip and sample where Φ is the work function and d is the tip–sample separation. In this scheme the sample is biased negative with respect to the tip and electrons tunnel from filled sample to empty tip states.

techniques.[7,8] These methodologies have provided important insight into the electronic and structural effects of doping; however, it is important to recognize that such techniques probe a macroscopic portion of a sample and thus provide an average picture of the solid. It is, however, also essential to characterize the electronic and structural properties of doped materials at the atomic level since modified materials often possess localized defects, structural disorder, and spatially inhomogeneous electronic structure.[9] A new technique that has begun to provide this key local information is scanning tunneling microscopy (STM).[10,11] In our discussion below we introduce STM and then describe several exciting results obtained with this technique in studies of the charge density wave phases of metal-substituted tantalum dichalcogenides.

The STM Experiment

The underlying basis for STM is electron tunneling between a sharp metal tip and a conducting sample.[11] When the tip and sample are brought sufficiently close (i.e., 5–10 Å apart), their wave functions can overlap. If a bias voltage is then applied to the sample, an electron tunneling current will flow between the sample and tip. The electrons tunnel from filled electronic states in the sample to empty states in the tip when the sample versus tip voltage is negative, and from the tip to empty sample electronic states when the bias is positive (Figure 1). The tunneling current depends exponentially on the tip–sample separation with a typical change of 10 per Å and also depends on the density of sample and tip electronic states.[11] The exponential distance dependence gives STM exquisite vertical sensitivity (ca. 0.01 Å); however, to image an interface at the atomic level also requires that the tip be scanned over the surface with angstrom resolution. Atomic-resolution x–y–z motion of the tip is accomplished by using piezoelectric positioners. A schematic diagram of the essential instrumental components is shown in Figure 1.

The most common method used to image a surface by STM is the constant-current mode.[11] In this mode of operation a feedback circuit controls the vertical (z) position of the tip above the sample so that the experimental tunneling current (I_t) is equal to a setpoint value (I_{ref}) at all x,y coordinates on the surface (Figure 1). Topographical features in an image thus correspond to the z displacement of the piezo. Theoretically, the constant-current-mode images have a straightforward interpretation as contours of constant local density of sample electronic states.[12,13] Hence, the STM experiment directly probes the sample electronic states near the Fermi level, and importantly, it is these states that play a key role in determining the conducting properties and reactivity of solids.

STM and Low-Dimensional Materials

As discussed above, STM is a surface-sensitive technique, and thus one might question whether it can provide information relevant to understanding the properties of bulk materials. For low-dimensional materials, such as layered solids, the surface is often structurally and electronically similar to the bulk,[15] and in these cases STM is an extraordinarily useful experimental probe. The similarity of bulk and surface is due to the low free energy of the van der Waals cleavage planes present in many low-dimensional materials; i.e., van der Waals surfaces do not reconstruct in contrast to the surfaces of three-dimensional covalent solids such as Si.[16] Of greater fundamental importance is the fact that low-dimensional materials are susceptible to interesting temperature-dependent instabilities, including metal/charge density wave (CDW) and metal/superconductor transitions.[17–20] Below we focus on CDWs in tantalum disulfide.

(7) Cheetham, A. K.; Day, P. *Solid State Chemistry: Techniques*; Clarendon Press: Oxford, 1987.
(8) Woodruff, D. P.; Delchar, T. A. *Modern Techniques of Surface Science*: Cambridge University Press: New York, 1986.
(9) Wu, X. L.; Zhang, Z.; Wang, Y. L.; Lieber, C. M. *Science* **1990**, *248*, 1211.
(10) Binnig, G.; Rohrer, H.; Gerber, C.; Weibel, E. *Phys. Rev. Lett.* **1982**, *49*, 57.
(11) For review, see: (a) Binnig, G.; Rohrer, H. *Angew. Chem., Int. Ed. Engl.* **1987**, *26*, 606. (b) Hansma, P. K.; Tersoff, J. *J. Appl. Phys.* **1987**, *61*, R1. (c) Hansma, P. K.; Elings, V. B.; Marti, O.; Bracker, C. E. *Science* **1988**, *242*, 157. (d) Kuk, Y.; Silverman, P. J. *Rev. Sci. Instrum.* **1989**, *60*, 165.
(12) (a) Tersoff, J.; Hamann, D. R. *Phys. Rev. Lett.* **1983**, *50*, 1998. (b) Tersoff, J.; Hamann, D. R. *Phys. Rev. B* **1985**, *31*, 805.
(13) This theory, which assumes that the density of tip states is constant, provides a good starting point for interpretation of images, although the tip electronic structure can play an important role.[14]
(14) (a) Tersoff, J. *Phys. Rev. B* **1990**, *41*, 1235. (b) Ciraci, S.; Baratoff, A.; Batra, I. P. *Phys. Rev. B* **1990**, *41*, 2763.
(15) (a) Wu, X. L.; Lieber, C. M. *Prog. Inorg. Chem.*, in press. (b) Balchin, A. A. *Crystallography and Crystal Chemistry of Materials With Layered Structures*; Levy, F., Ed.; D. Reidel Publishing Company: Boston, 1976; p 1.
(16) Zangwill, A. *Physics at Surfaces*; Cambridge University Press: New York, 1988.
(17) Rouxel, J. *Crystal Chemistry and Properties of Materials with Quasi-One-Dimensional Structures*; D. Reidel Publishing Company: Boston, 1986; p 1.
(18) DiSalvo, F. J.; Rice, M. T. *Phys. Today* **1979**, April, 32.
(19) (a) DiSalvo, F. J. In *Electron-Phonon Interactions and Phase Transitions*; Riste, T., Ed.; Plenum: New York, 1977; p 107. (b) Wilson, J. A.; DiSalvo, F. J.; Mahajan, S. *Adv. Phys.* **1975**, *24*, 117.
(20) Withers, R. L.; Wilson, J. A. *J. Phys. C: Solid State Phys.* **1986**, *19*, 4809.

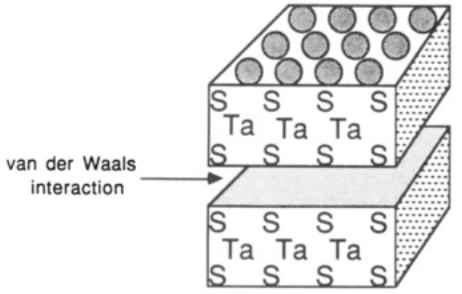

Figure 2. Schematic view of two S–Ta–S layers of TaS_2 that interact with each other through van der Waals forces. The sulfur atoms are arranged in hexagonally close packed planes.

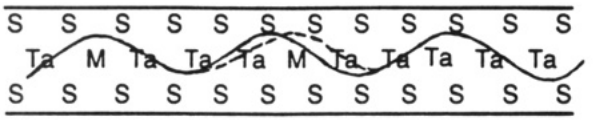

Figure 3. Schematic view of a single layer of TaS_2 with one metal impurity, M. The solid curve represents an undistorted CDW, and the dashed curve indicates a possible distortion of the CDW due to the metal impurity.

Metal-Substituted TaS_2 and Charge Density Waves

Tantalum disulfide is a layered material that consists of strongly bonded sulfur–tantalum–sulfur layers that are held together by weak van der Waals interactions between adjacent hexagonally packed sulfur planes (Figure 2).[15,19] The tantalum centers can be coordinated in either octahedral (1T-TaS_2) or trigonal prismatic (2H-TaS_2) holes between the sulfur planes; herein, we focus exclusively on 1T-TaS_2. Electronically, one would expect that the partially filled t_{2g} conduction band in this d^1 system would give rise to metallic conduction. At high temperatures TaS_2 is indeed metallic; however, on cooling below 543 K, TaS_2 exhibits four distinct temperature-dependent CDW states.[19] In general, CDWs are found in low-dimensional systems that exhibit significant Fermi surface nesting, where nesting refers to the condition that a piece of Fermi surface may be translated and superimposed on another piece by a wave vector **q**. Fermi surface nesting leads to a divergence in the electronic susceptibility at the wave vector **q** and, through electron–phonon coupling, can yield a stable periodic modulation of the lattice and conduction electron density, that is, a CDW. The periodicity or wavelength (λ) of the CDW is governed by **q**. Since λ is determined by the Fermi surface size through **q**, it may not correspond to an integral number of lattice constants ($n\mathbf{a}$). In the case where $\lambda \neq n\mathbf{a}$, the CDW is called incommensurate; however, when $\lambda = n\mathbf{a}$, it is termed commensurate.[21]

Prior to the advent of STM, the structure of the CDW phases in TaS_2 and other materials had been investigated by X-ray and electron diffraction techniques. These techniques showed in TaS_2 that the high-temperature CDW was incommensurate and that for $T < 183$ K the CDW rotated 13.9° relative to the atomic lattice to become commensurate.[19,20] Additionally, diffraction studies indicated that a cluster of 13 Ta atoms, which corresponds to the periodic lattice distortion, could be associated with each CDW maximum. Unfortunately, it was not possible to resolve the structures of the two intermediate-temperature CDW phases by diffraction techniques. This situation has changed substantially since it was shown that STM could directly image a CDW.[22] The ability of STM to determine simultaneously both CDW and atomic lattice positions has subsequently been exploited by us[23,24] and

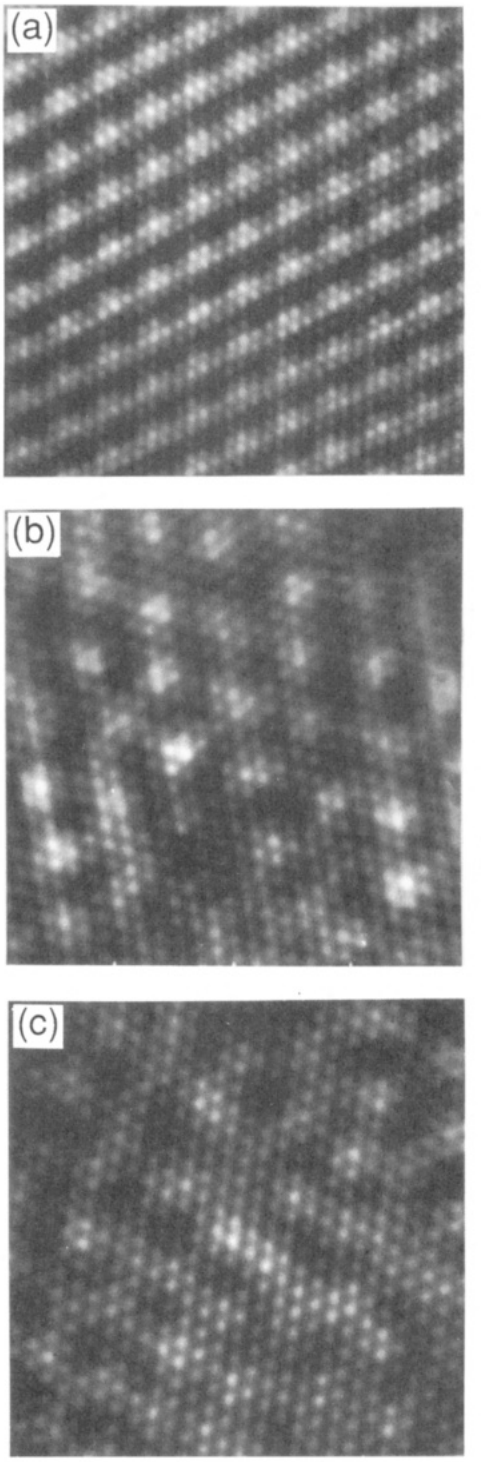

Figure 4. Gray-scale images of the incommensurate CDW phase of (a) TaS_2, (b) $Ti_{0.08}Ta_{0.92}S_2$, and (c) $Ti_{0.2}Ta_{0.8}S_2$ recorded at 360, 300, and 300 K, respectively. Image a is 100 × 100 Å^2, and images b and c are 80 × 80 Å^2.

(21) A commensurate CDW may have $\lambda \neq n\mathbf{a}$ when it is rotated relative to the lattice. In this case the commensurate period can be calculated by simple geometry.

(22) Coleman, R. V.; Drake, B.; Hansma, P. K.; Slough, G. *Phys. Rev. Lett.* **1985**, *55*, 394.

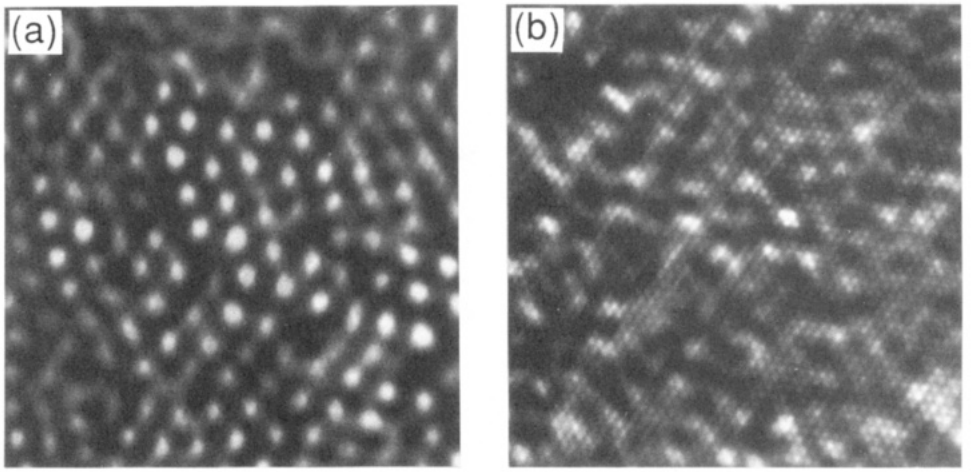

Figure 5. Gray-scale images, 150 × 150 Å^2, of (a) $Fe_{0.04}Ta_{0.96}S_2$ and (b) $Fe_{0.15}Ta_{0.85}S_2$ recorded at room temperature.

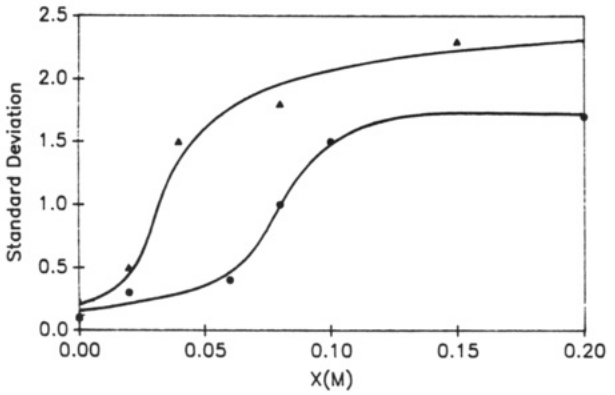

Figure 6. Plots of the standard deviation (σ) in angstroms for the CDW wavelength as a function of x(Ti) (●) and x(Fe) (▲). λ for TaS_2 is 11.8 Å.

others[25,26] to resolve the complicated structural details of the intermediate-temperature CDW phases in TaS_2. These data promise to increase significantly our understanding of the physics of this material.

Another fundamental problem of greater chemical interest is to understand how a CDW interacts with a metal impurity doped into the lattice (Figure 3); such information is essential if one wishes to modify the properties of this or other systems in a predictable manner. Previously, the effects of metal substitution on the CDW phases in metal-substituted tantalum disulfide, $M_xTa_{1-x}S_2$, have been probed by diffraction and transport measurements.[6,19] These studies showed that metal impurities drive the CDW to the incommensurate state. In general, these observations are consistent with a random impurity potential which decreases and ultimately eliminates the electrostatic energy gained from the periodic CDW–lattice interaction in the commensurate and nearly commensurate states.[19,20,27] The detailed structure of the incommensurate phase in the $M_xTa_{1-x}S_2$ materials could not be determined from the diffraction studies, although this information is essential for developing a microscopic understanding of these systems. Indeed, our recent STM studies of $M_xTa_{1-x}S_2$ materials (M = Ti, Fe, Nb) have shown that the atomic level response of the CDW phase to metal impurities is significantly more complicated than previously predicted.[28-33]

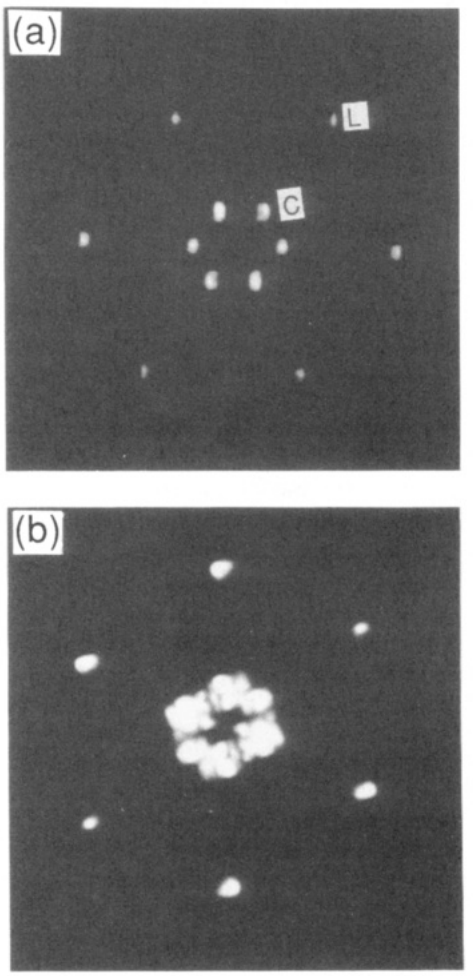

Figure 7. Two-dimensional Fourier transform power spectra of images of (a) TaS_2 and (b) $Ti_{0.1}Ta_{0.9}S_2$. The first-order atomic lattice (L) and CDW peaks (C) are marked in spectrum a.

(23) Wu, X. L.; Lieber, C. M. *Science* **1989**, *243*, 1703.
(24) (a) Wu, X. L.; Lieber, C. M. *Phys. Rev. Lett.* **1990**, *64*, 1150. (b) Wu, X. L.; Lieber, C. M. *J. Vac. Sci. Technol.* **1991**, *B9*, 1044. (c) Wu, X. L.; Lieber, C. M., submitted for publication.
(25) Thomson, R. E.; Walter, U.; Ganz, E.; Clarke, J.; Zettl, A.; Rauch, P.; DiSalvo, R. *J. Phys. Rev. B* **1988**, *38*, 10734.
(26) (a) Giambattista, B.; Slough, C. G.; McNairy, W. W.; Coleman, R. V. *Phys. Rev. B* **1990**, *41*, 10082. (b) Slough, C. G.; McNairy, W. W.; Coleman, R. V.; Garnaes, J.; Prater, C. B.; Hansma, P. K. *Phys. Rev. B* **1990**, *42*, 9255.
(27) McMillan, W. L. *Phys. Rev. B* **1975**, *12*, 1187.

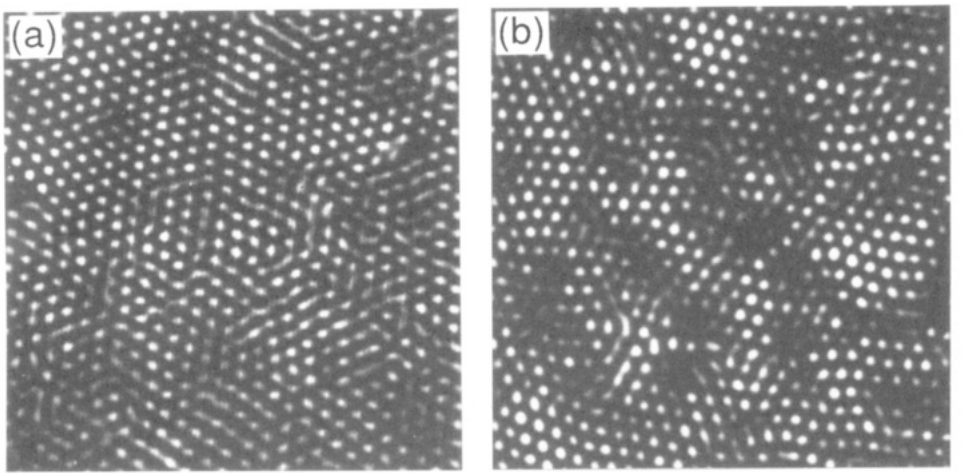

Figure 8. Images, 300 × 300 Å^2, of (a) $Nb_{0.04}Ta_{0.96}S_2$ and (b) $Nb_{0.07}Ta_{0.93}S_2$ recorded at 340 and 315 K, respectively.

Strong-Pinning Metal Centers

In studies of Ti-substituted tantalum disulfide materials, $Ti_xTa_{1-x}S_2$, we have shown that the randomly substituted titanium centers significantly disorder the CDW superlattice (Figure 4).[28,29] The hexagonal atomic lattice (period = 3.35 Å) and the CDW modulation are simultaneously resolved in these images. Macroscopic measurements made on these crystals suggest that the CDW phase of the pure and doped samples is incommensurate at the temperature of the STM experiment; however, visual inspection of the images indicates that the incommensurate phase of $Ti_{0.08}Ta_{0.92}S_2$ and $Ti_{0.2}Ta_{0.8}S_2$ is significantly less regular than in pure TaS_2. Since the hexagonal atomic lattice is periodic regardless of x(Ti), we know that the distortions in the CDW are due not to imaging artifacts but rather to the Ti impurities in the lattice. Distortions in the CDW superlattice of the incommensurate phase are also observed in images of $Fe_xTa_{1-x}S_2$ materials (Figure 5),[30,31] and thus it appears that substitution of nonisoelectronic metals will in general induce large distortions in the CDW. These STM experiments thus give us a substantially more detailed picture of the CDW structure in metal-doped compounds than previous diffraction investigations.

To quantify and understand this disorder in the CDW structure, we have employed several distinct methods. In early work we found that a direct measure of the CDW distortions is the standard deviation (σ) of the CDW wavelength (λ) determined from analysis of the real-space images.[29] The data for the Ti- and Fe-substituted materials indicate that the magnitude of the CDW distortions increases as the concentration of metal impurities increases with σ increasing more rapidly in the $Fe_xTa_{1-x}S_2$ versus the $Ti_xTa_{1-x}S_2$ series (Figure 6). Since disorder in the lattice potential also increases with the concentration of substituted Ti or Fe, we have suggested that the CDW distortions, which approach 2 Å at high substitution levels, are driven by the random lattice potential.[29,31] Furthermore, the localized nature of these distortions indicates that the CDW–impurity interaction is strong, and hence Ti and Fe are examples of strong-pinning impurities.[34]

It is also interesting that there are sharp increases in the σ versus x(M) curves at x(Fe) $\approx$ 0.03 and x(Ti) $\approx$ 0.08 (Figure 6). Since Fe substitutes as Fe(II)[35] and oxidizes two tantalum centers to d^0-Ta(V) to maintain charge neutrality, a total of three impurities can be associated with each Fe center. Thus, substitution levels of 0.03 for Fe and 0.08 for Ti correspond to a similar total impurity concentration. As previously pointed out, these doping levels correspond to 1 impurity/CDW maximum since there are 13 metal lattice sites associated with each CDW maximum. We have suggested that 1-impurity/CDW maximum represents a critical concentration for TaS_2 at which the CDW–impurity interaction energy is greater than the energy to distort and localize the CDW superlattice.[31] Furthermore, for nonisoelectronic metal impurities it is apparent that the critical concentration is independent of the chemical identity of the impurity. Evidence for this critical concentration is also found in macroscopic transport measurements which show that the nearly commensurate and commensurate CDW phases are completely suppressed above 1 impurity/CDW maximum.[6] In the future it will be interesting to probe directly the density of electronic states by scanning tunneling spectroscopy in these $M_xTa_{1-x}S_2$ materials for x(M) near the 1 impurity/CDW maximum critical point. We predict that the increased distortions and localization observed above this critical concentration should be reflected in a decrease in the density of states near the Fermi level.

To understand differences in CDW structure for metal-substituted materials in our STM studies versus previous diffraction investigations, we have used two-dimensional Fourier transform (2DFT) power spectra calculated from the images (Figure 7).[31] The 2DFT power spectrum corresponding to an image of a pure TaS_2 sample exhibits two sets of sharp spots that correspond to the first-order CDW and lattice peaks expected for a regular superlattice. The metal-substituted compounds show diffuse intensity around the CDW positions, and the spread of this diffuse intensity increases with x(M). Diffuse scattering observed in diffraction studies has been attributed to possible fluctu-

(28) Wu, X. L.; Zhou, P.; Lieber, C. M. *Nature (London)* **1988**, *335*, 55.
(29) Wu, X. L.; Zhou, P.; Lieber, C. M. *Phys. Rev. Lett.* **1988**, *61*, 2604.
(30) Chen, H.; Lieber, C. M. *Proc. Air Force Tribol. Tech. Rev.*, in press.
(31) Chen, H.; Wu, X. L.; Lieber, C. M. *J. Am. Chem. Soc.* **1990**, *112*, 3326.
(32) Wu, X. L.; Lieber, C. M. *J. Am. Chem. Soc.* **1989**, *111*, 2731.
(33) Dai, H.; Chen, H.; Lieber, C. M. *Phys. Rev. Lett.*, in press.

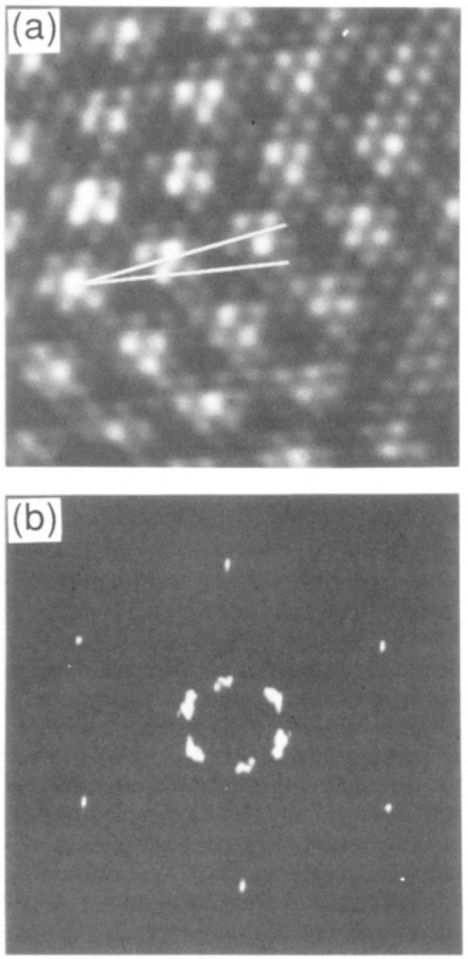

Figure 9. (a) Atomic resolution image, 58 × 58 Å^2, of $Nb_{0.04}Ta_{0.96}S_2$ illustrating the rotation of a CDW domain relative to the lattice. (b) 2DFT power spectra of $Nb_{0.04}Ta_{0.96}S_2$.

ations in the hexagonal incommensurate phase;[20] however, from our real-space and 2DFT measurements it is clear that the diffuse scattering should be attributed to random variations in the CDW wavelength due to impurity pinning. We thus conclude that 2DFT power spectra can provide an important link between real-space images obtained directly by STM and more conventional reciprocal-space diffraction analyses.

A final method that we have begun to explore in analyzing the STM images of these $M_xTa_{1-x}S_2$ materials and other disordered solids is based on calculation of translational and orientational correlation functions. Such statistical analyses can provide unique insight into the nature of disorder as will be shown below.

Weak-Pinning Metal Centers

In the metal-substituted systems described above, the nonisoelectronic impurities (Ti, Fe) cause significant localized distortions of the CDW and thus correspond to strong-pinning centers. In addition to a strong-pinning regime of CDW–impurity interaction, there has been considerable interest in the so-called weak-pinning regime. Weak pinning of CDWs was first discussed by Fukuyama, Lee, and Rice (FLR), who proposed that the CDW will break up into constant-phase domains that contain more than one impurity.[34] The average CDW

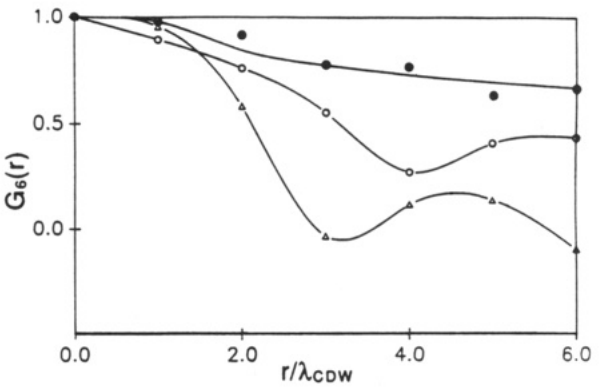

Figure 10. Plots of the orientational correlation function $G_6(r)$ calculated from images of $Nb_{0.04}Ta_{0.96}S_2$ (●), $Nb_{0.07}Ta_{0.93}S_2$ (○), and $Nb_{0.1}Ta_{0.9}S_2$ (△), where λ_{CDW} is the CDW period.

phase within a given domain adjusts to the random impurity potential to maximize the average CDW–impurity interaction in contrast to the local CDW–impurity interaction for the strong-pinning case. This weak-pinning model has been controversial,[36,37] and indeed some recent theoretical work suggests that pinning will always be strong.[37] Unfortunately, there is little structural data that addresses the weakly pinned regime. This is not unexpected since the predicted random-phase CDW domains would be difficult to identify by the diffraction methods.

In STM studies of the incommensurate CDW in niobium-substituted TaS_2 we have found strong evidence for the FLR weak-pinning regime.[33] Images of $Nb_xTa_{1-x}S_2$ materials exhibit constant-phase domains that are rotated relative to each other; i.e., the CDW phase differs in adjacent domains (Figure 8). Assuming roughly circular domains, we showed that the domain diameter decreases from ≈72 to 42 Å as x(Nb) increases from 0.04 to 0.07 and that the domains contain on average at least 10 impurities. These results are consistent with predictions from weak-pinning models.[34]

Real- and reciprocal-space analyses of atomic resolution images has provided considerable insight into the local structure of these niobium-doped materials. The CDW maxima within "domains" are rotated relative to the atomic lattice in contrast to pure TaS_2; the CDW–lattice angle is typically found to vary within ±15° (Figure 9). Such rotations suggest that CDW domains are stabilized by adjusting their phase (i.e., rotation of one or more CDW wave vectors) to maximize the average CDW–impurity interaction. 2DFT analyses of the real-space data are consistent with this explanation and also highlight the significant difference between Nb and the strong-pinning impurities Ti and Fe (Figure 9). The CDW peaks in the 2DFT power spectra show angular elongation which corresponds to clockwise and counterclockwise rotations of the CDWs relative to the lattice as expected from the real-space images. The radial broadening of the CDW peaks is much smaller than observed for Ti- and Fe-substituted TaS_2, and thus we conclude that the CDW wavelength is not grossly distorted in $Nb_xTa_{1-x}S_2$.

In addition, we have recently noted that the 2DFT power spectra are very similar to the structure factors observed for the "hexatic" phase of several two-dimen-

(34) (a) Fukuyama, H.; Lee, P. A. *Phys. Rev. B* **1978**, *17*, 535. (b) Lee, P. A.; Rice, T. M. *Phys. Rev. B* **1979**, *19*, 3970.
(35) Eibschutz, M.; DiSalvo, F. J. *Phys. Rev. Lett.* **1976**, *36*, 104.
(36) Coppersmith, S. N. *Phys. Rev. Lett.* **1990**, *65*, 1044.
(37) Tucker, J. R. *Phys. Rev. B* **1989**, *40*, 5447.

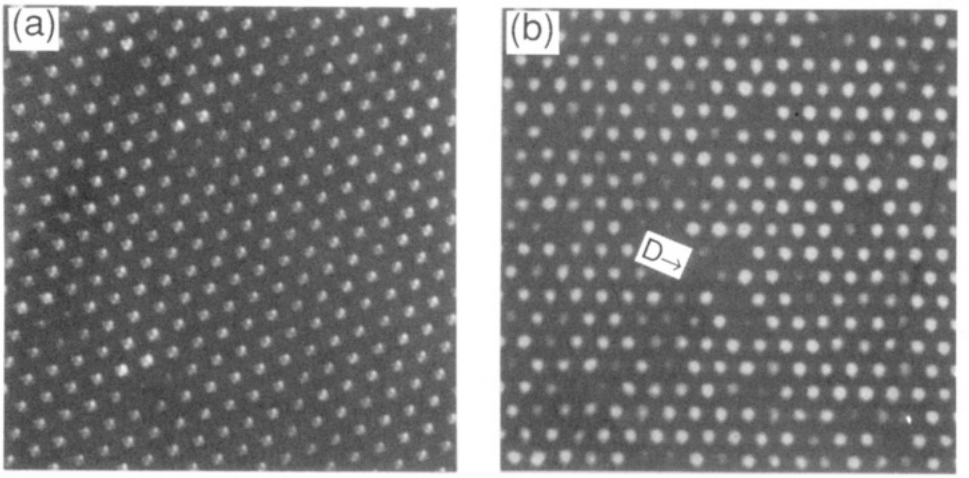

Figure 11. Images, 220 × 220 Å^2, of (a) $TaSe_2$ and (b) $Ti_{0.04}Ta_{0.96}S_2$. A CDW defect is marked (D) in image b.

sional systems.[38-40] This distinct phase of matter was predicted theoretically by Nelson several years ago and corresponds to a system that has structural order between that of liquid and crystalline phases of matter.[40] The hexatic phase characteristically shows long-range orientational order but only short-range translational order.

To investigate the orientational order of the incommensurate CDW phase in $Nb_xTa_{1-x}S_2$ materials, we have calculated the orientational correlation function $G_6(r)$ for the orientational order parameter $\varphi_6(r) = \sum\exp(i6\Phi_j)$ (Figure 10).[38,40] Previous studies have shown that the long-range orientational order of a hexatic phase will have a power law decay in $G_6(r)$, while $G_6(r)$ will decay exponentially in amorphous or liquid phases. Our calculated decay of $G_6(r)$ for $x(\text{Nb}) = 0.04$ can be fit to a power law decay, $r^{-\eta}$, with $\eta \approx 0.2$. This value for the decay constant is consistent with the hexatic phase close to the hexatic–liquid phase transition, $\eta = 0.25$. For $x(\text{Nb}) = 0.07$ and 0.10 samples, $G_6(r)$ has oscillations, which are due in part to insufficient averaging;[41] however, the CDW orientational order obviously decreases from $x = 0.04$ to 0.10. Notably, these results show that (1) calculation of the orientational and translational correlation functions is an important new method for quantifying disorder in STM images and (2) impurity-induced disorder in this CDW system gives rise to an intermediate state of matter, the hexatic phase, which has been observed in other two-dimensional systems.

Impurities and the Commensurate CDW Phase

In the studies discussed above, we focused on how impurities (Ti, Fe, and Nb) pin or interact with an incommensurate CDW. We have also studied the effects of impurities on a commensurate CDW. The commensurate CDW–impurity interaction is expected to be quite distinct from that discussed above since the CDW is already pinned to the lattice in the commensurate state. Indeed, McMillan's theoretical studies indicate that while the incommensurate state is stabilized by impurity pinning, the commensurate state remains essentially unchanged.[27]

To investigate the nature of the commensurate CDW–impurity interaction, we have studied metal-substituted tantalum diselenide.[42] Images of Ti-substituted $TaSe_2$, $Ti_xTa_{1-x}Se_2$, show that the CDW superlattice maintains a regular commensurate structure (similar to the pure material), although there are also localized regions where the CDW amplitude is reduced relative to the rest of the image (Figure 11). We have termed these localized regions "CDW defects". Analysis of the concentration dependence and structure of the defects has shown that it is an amplitude distortion that relaxes the CDW around titanium impurities. The very localized nature of these defects also indicates that tunneling spectroscopy measurements should be able to characterize changes in the density of states due to the CDW–Ti interaction. Such data, which can only be obtained directly by STM, will be essential for quantifying the CDW–impurity interaction.

Lastly, we have found in these studies that at higher titanium concentrations ($x \geq 0.07$) the CDW defects exhibit a coupled amplitude–phase distortion. The nature of the phase distortion is highly specific (in contrast to that of the incommensurate state) and yields CDW twin domains.[42] 2DFT analyses of this data show the expected splitting of the first-order CDW peaks (seen previously in diffraction); however, the real-space STM data have shown for the first time the origin and detailed structure of the domain boundaries.

Conclusions and Future Prospects

In the studies described above we have illustrated how the high-resolution real-space information provided by STM can provide unique insight into understanding the interaction of metal impurities with the CDW phases in tantalum dichalcogenide materials. In this work STM was used primarily as a structural technique, although our results also indicate that impurities affect the electronic states significantly. In the future it will be important to characterize the density of electronic states that are associated with impurity-induced phase transitions and defects. This latter data is readily available from tunneling spectroscopy measurements.

(38) Nelson, D. R.; Rubinstein, M.; Spaepen, F. *Philos. Mag. A* **1982**, *46*, 105.
(39) Murray, C. A.; Van Winkle, D. H. *Phys. Rev. Lett.* **1987**, *58*, 1200.
(40) Nelson, D. R.; Halperin, B. I. *Phys. Rev. B* **1979**, *19*, 2457.
(41) Dai, H.; Lieber, C. M., unpublished results.
(42) Wu, X. L.; Lieber, C. M. *Phys. Rev. B* **1990**, *41*, 1239.

In a broader sense, it is clear that STM can provide key insight into understanding the atomic level properties of other interesting and important low-dimensional materials. For example: (1) new and fascinating electronic properties of graphite intercalation compounds have recently been elucidated by us[43] and other groups;[44] (2) additionally, STM is providing essential data on the structural and electronic properties of high-temperature copper oxide superconductors and how these properties evolve locally upon metal and oxygen doping.[9,45,46] These and other studies will undoubtedly lead to significant advances in our understanding of these materials in the future.

We acknowledge our co-workers whose efforts are referenced in this account and the Air Force Office of Scientific Research, National Science Foundation, David and Lucile Packard Foundation, A. P. Sloan Foundation, and Camile and Henry Dreyfus Foundation for financial support.

(43) (a) Kelty, S. P.; Lieber, C. M. *J. Phys. Chem.* **1989**, *93*, 5983. (b) Kelty, S. P.; Lieber, C. M. *Phys. Rev. B* **1989**, *40*, 5856. (c) Kelty, S. P.; Lieber, C. M. *J. Vac. Sci. Technol.* **1991**, *B9*, 1068.
(44) Anselmetti, D.; Wiesendanger, R.; Guntherodt, H.-J. *Phys. Rev. B* **1989**, *39*, 11135.
(45) Zhang, Z.; Wang, Y. L.; Wu, X. L.; Huang, J.-L.; Lieber, C. M. *Phys. Rev. B* **1990**, *42*, 1082.
(46) (a) Zhang, Z.; Wang, Y. L.; Wu, X. L.; Huang, J.-L.; Lieber, C. M. *Proc. World Congr. Supercond. Houston, 1990.* (b) Wu, X. L.; Wang, Y. L.; Zhang, Z.; Lieber, C. M. *Phys. Rev. B* **1991**, *43*, 8729.

Magnetic and Spin Effects in Photoreduction of Uranyl Salts

ANATOLY L. BUCHACHENKO and IGOR V. KHUDYAKOV*,†

Institute of Chemical Physics, Academy of Sciences of the USSR, 117977 Moscow, USSR

Received August 3, 1990 (Revised Manuscript Received April 8, 1991)

A remarkable feature of spin-selective chemical reactions is their magnetic sensitivity. This sensitivity arises from magnetic interactions of electrons and nuclei with an external magnetic field and also from electron–nuclear hyperfine interactions. From an energy standpoint these magnetic interactions are negligible, but they nevertheless influence the overall chemistry by reorienting electron spins and removing spin prohibition in a spin-selective reaction. Spin prohibition means that not all spin states are reactive; only reactions in which electron spin is conserved are allowed. Magnetic interactions can remove the spin prohibition and thereby strongly influence the rate and efficiency of certain chemical reactions. Well-established magnetic effects include chemically induced dynamic nuclear and electron polarizations (CIDNP and CIDEP), magnetic field effects (MFE; an external magnetic field influences reaction rates), and magnetic isotope effects (MIE).[1] The MIE is the most interesting because it reflects the reaction-rate dependence of paramagnetic particles on the spin and magnetic moments of their nuclei.[2] This rate dependence provides a basis for separation of magnetic and nonmagnetic isotopes in chemical reactions, and it has been observed for isotopes of carbon,[3] oxygen,[4] silicon,[5] and sulfur.[6,7]

The following reaction scheme has been found successful for analysis of most isotope separation processes.[2] Reagent A/A# containing magnetic (A#) and nonmagnetic isotopes (A) is photoexcited and then reacts in the triplet state ($^3A^*$; Scheme I). A triplet radical pair (RP) is formed $^3[R_1^\bullet, R_2^\bullet]$. The RP can

Scheme I[a]

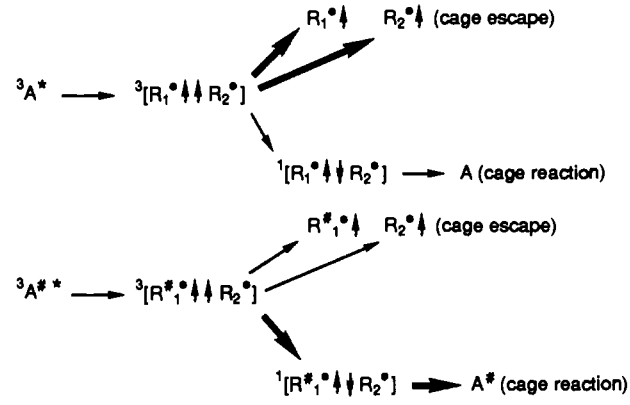

[a] Square brackets denote the solvent cage.

Anatoly L. Buchachenko was born in 1935. He graduated from Gorki State University in 1958. Currently he is Professor and Laboratory Head of the Institute of Chemical Physics at the Academy of Sciences of the USSR. He is also a member of the Academy of Sciences of the USSR. He is an expert in the physics and chemistry of free radicals and in the theory of radical reactions and chemical reactivity.

Igor V. Khudyakov was born in Moscow in 1949. He graduated from Moscow State University in 1971 and since then has been an officer in the Institute of Chemical Physics at the Academy of Sciences of the USSR. He was awarded a Ph.D. in 1975 and D.Sc. in 1984 and is currently Research Fellow and Professor. His scientific interests include fast reactions of free radicals in solution, magnetic field effects in chemical reactions, and photochemistry.

† Present address: Department of Chemistry, Columbia University, New York, NY 10027.

(1) For reviews, see: (a) Salikhov, K. M.; Molin, Y. N.; Sagdeev, R. Z.; Buchachenko, A. L. *Spin. Polarization and Magnetic Effects in Radical Reactions*; Elsevier: Amsterdam, 1984. (b) Steiner, U. E.; Ulrich, T. *Chem. Rev.* **1989**, *89*, 51. (c) Gould, I. R.; Turro, N. J.; Zimmt, M. B. *Adv. Phys. Org. Chem.* **1984**, *20*, 1.
(2) (a) Buchachenko, A. L. *Prog. React. Kinet.* **1984**, *13*, 164. (b) Turro, N. J.; Kraeutler, B. In *Isotopic Effects: Recent Developments in Theory and Experiment*, Vol. 6 of *Isotopes in Organic Chemistry*; Elsevier: Amsterdam, 1984; p 107.
(3) Buchachenko, A. L.; Galimov, E. M.; Ershov, V. V.; Nikiforov, G. A.; Pershin, A. D. *Dokl. Akad. Nauk SSSR* **1976**, *228*, 379.
(4) Buchachenko, A. L.; Fedorov, A. V.; Yasina, L. L.; Galimov, E. M. *Chem. Phys. Lett.* **1984**, *103*, 405.
(5) Step, E. N.; Tarasov, V. F.; Buchachenko, A. L. *Izv. Akad. Nauk SSSR, Ser. Khim.* **1988**, 200; **1988**, 2250.
(6) Step, E. N.; Tarasov, V. F.; Buchachenko, A. L. *Nature* **1990**, *346*, No. 6270, 25.
(7) An earlier reference for the MIE in tin is mentioned here: (a) Podoplelov, A. V.; Leshina, T. V.; Sagdeev, R. Z.; Molin, Y. N.; Goldanski, V. I. *Pis'ma. Zh. Eksp. Teor. Fiz.* **1979**, *29*, 419. (b) Podoplelov, A. V.; Sen Chel Su; Sagdeev, R. Z.; Shtein, M. S.; Moralev, V. M.; Goldanski, V. I.; Molin, Y. N. *Izv. Akad. Nauk SSSR, Ser. Khim.* **1985**, 2207. Clear evidence for a ^{117,119}Sn MIE has not been found.

0001-4842/91/0124-0177$02.50/0